

Dependence of planar alignment layer upon enhancement of azimuthal anchoring energy by reactive mesogens

This content has been downloaded from IOPscience. Please scroll down to see the full text.

2015 Jpn. J. Appl. Phys. 54 011701

(<http://iopscience.iop.org/1347-4065/54/1/011701>)

View [the table of contents for this issue](#), or go to the [journal homepage](#) for more

Download details:

IP Address: 166.104.145.58

This content was downloaded on 02/02/2016 at 04:45

Please note that [terms and conditions apply](#).

Dependence of planar alignment layer upon enhancement of azimuthal anchoring energy by reactive mesogens

Youngsik Kim^{1†}, You-Jin Lee^{2†}, Ji-Ho Baek¹, Chang-Jae Yu^{1,2}, and Jae-Hoon Kim^{1,2*}

¹Department of Information Display Engineering, Hanyang University, Seoul 133-791, Korea

²Department of Electronic Engineering, Hanyang University, Seoul 133-791, Korea

E-mail: jhoon@hanyang.ac.kr

Received August 26, 2014; accepted October 8, 2014; published online December 4, 2014

Reactive mesogens (RMs) can enhance the azimuthal anchoring energy of planar alignment layers used in liquid crystal (LC) devices; herein, we studied the interactions between the RMs and the planar alignment material that determine whether this enhancement can occur. Two alignment-layer materials were studied: polyamic acid (PA) and polyimide (PI). The addition of RMs to the PI-type alignment layer was effective in enhancing the azimuthal anchoring energy, whereas the addition of RMs to the PA-type alignment layer had little effect. Surface analysis revealed that the RMs adhered well to the PI-type alignment surface only; in the resulting cell, the presence of the RMs enhanced both the rise and decay times in fringe field switching (FFS)-mode operation. © 2015 The Japan Society of Applied Physics

1. Introduction

Surface anchoring energy is of great importance to the understanding of the interfacial phenomena in liquid crystal (LC) devices, such as their surface ordering, surface transitions, and performance.¹⁻⁴ Surface anchoring energy is classified into two types on the basis of the Rapini-Papoular model for surface free energy.⁵ One is the polar anchoring energy, which is defined as the out-of-plane motion of LC molecules away from the substrate surface, and the other is the azimuthal anchoring energy, which is defined as the in-plane motion of LC molecules. Because the surface anchoring energy is related to the alignment stability of LCs under static conditions and to the switching behavior under dynamic conditions, many researchers have investigated ways to enhance the surface anchoring energy.⁶⁻⁹

Recently, the addition of UV-curable reactive mesogens (RMs) to LCs was proposed to increase the azimuthal anchoring energy. RM polymers provide volume stability to LC molecules as well as strong molecular interactions, and thus their addition has enhanced the azimuthal anchoring energy, improving the response time characteristics in in-plane switching (IPS) and fringe field switching (FFS) modes.^{10,11} In this method, the RM monomers remaining within the LC layer after UV polymerization reduce the display performance owing to, for example, the image sticking problem. In our previous works, we reported that RMs coated upon or mixed into the planar alignment layer greatly increased the azimuthal anchoring energy, leading to fast response times of cells operated in the FFS mode.¹² However, the influences of alignment materials on the azimuthal anchoring energy and the response time have not been studied in this material system.

In this work, we studied the interactions between the planar alignment layer material and the RMs that determine whether the RMs enhance the azimuthal anchoring energy; the surface anchoring energy of a polyimide (PI) alignment layer in which polymerized RMs were present was found to be greater than that of a PI alignment layer without RMs, and also greater than that of polyamic acid (PA) alignment layers regardless of whether polymerized RMs were present.

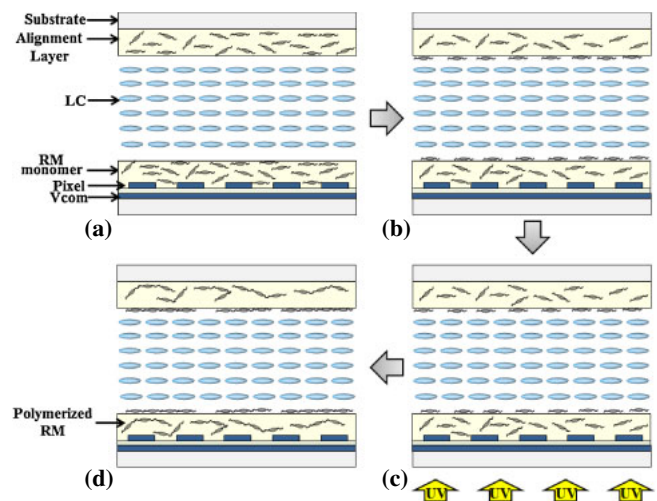


Fig. 1. (Color online) Schematic diagram of the fabrication process.

To explain the dependence of the effect on the alignment material used, we evaluated the surface properties through time-of-flight secondary ion mass spectrometry (TOF-SIMS) and atomic force microscopy (AFM). The enhanced surface anchoring energy was found to result from polymerized RMs present on the alignment layer; these RMs improved the response time characteristics of cells operated in the FFS mode.

2. Experimental methods

The fabrication processes used are illustrated schematically in Fig. 1. We fabricated a FFS cell. On the bottom substrate, the upper and lower indium-tin-oxide (ITO) layers were used as the pixel electrode with 3 μm width and 5 μm intervals and the common electrode without any pattern, respectively. The thicknesses of the ITO layer and the insulator layer, which is between the two electrode layers, were 40 and 400 nm, respectively. The top substrate had no electrode layer. On the two substrates, alignment materials were spin-coated and prebaked at 100 °C for 10 min, followed by curing at 210 °C for 2 h. We used two types of planar alignment materials: PA (Nissan Chemical SE2414) and PI (JSR AL16470). The planar alignment layer was mixed with the

[†]These authors contributed equally to this work.

RM material (Merck RM257, 2.0 wt%) and the photoinitiator IRGACURE 651 (Chiba Chemical, 20 wt% of RM); then, the surfaces were rubbed 7° to the electrode direction to predetermine the switching direction. The cell thickness was maintained using glass spacers of $2.7\ \mu\text{m}$ thickness; the cell was filled with LC material (Merck MLC0643, $\Delta n = 0.1023$ and $\Delta\epsilon = 6.9$) by capillary action at the isotropic phase temperature. In the cell's initial state, LC molecules were aligned along the rubbing direction on the alignment layer, and RM monomers were distributed randomly on the surface as well as in the bulk of the alignment layer, as shown in Fig. 1(a). Then, RM monomers reoriented themselves along the LC molecules, as shown in Fig. 1(b), because RM monomers were easily dissolved in the LCs and easily movable owing to the RM's liquid crystalline properties. To polymerize the RM monomers, they were exposed to $3.3\ \text{J}/\text{cm}^2$ of 365 nm UV light for 30 min; the resulting polymers followed the direction of the LC molecules on the surface and in the bulk of the alignment layer, as shown in Figs. 1(c) and 1(d).

The electrooptic properties of the FFS cells were measured using a He–Ne laser ($\lambda = 632.8\ \text{nm}$), a digitized oscilloscope (Tektronix TDS754D), two crossed polarizers, and a photodetector (THORLABS PDA55). The azimuthal anchoring energy was measured by means of the torque balance method.¹³⁾ The test cells were $5\ \mu\text{m}$ thick and were filled with MLC0643 mixed with chiral dopant (chiral pitch: $\pm 30\ \mu\text{m}$). The actual twist angle was obtained by rotating the analyzer and polarizer together in steps of 0.1° and noting the angle of minimum transmittance. TOF-SIMS was used for surface analysis of planar alignment layers with and without RMs; the instrument used was TOF.SIMS 5 (IonTOF) equipped with a bismuth (Bi) ion gun, operated at 25 keV with an ion current of 1.05 pA; the analysis spot size was $100\ \mu\text{m}$ in diameter. Charge neutralization was used to reduce the charging effect, and the surface morphologies of alignment layers with and without RMs were also observed by AFM (Park Systems XE-100).

3. Results and discussion

It is well known that the surface anchoring energy is mainly dependent on the chain ordering of the alignment material and the molecular interactions between the alignment layer and the LC molecules.¹⁴⁾ In particular, in cases where RM polymers are present on the surface of the planar alignment layer, these RM polymers cover the main chain of the alignment polymer and induce strong interactions with LC molecules, such as π – π stacking interactions or dipole–dipole interactions. The strong molecular interactions induced by the RM polymers enhance the azimuthal anchoring energy.¹⁵⁾

Figure 2 shows the measured azimuthal anchoring energy of the two types of alignment layer (PA- and PI-types), both with and without RMs. The addition of RMs to the PI-type alignment layer yielded an azimuthal anchoring energy approximately 175% that of the pure alignment layer. In contrast, the presence or absence of RMs had no apparent effect upon the azimuthal anchoring energy of the PA-type alignment layer, even though the same manufacturing processes were used. On the basis of these results, the enhancement of the azimuthal anchoring energy that can be achieved by adding RMs appears to depend strongly upon the kind of alignment layer. As mentioned before, the presence of the

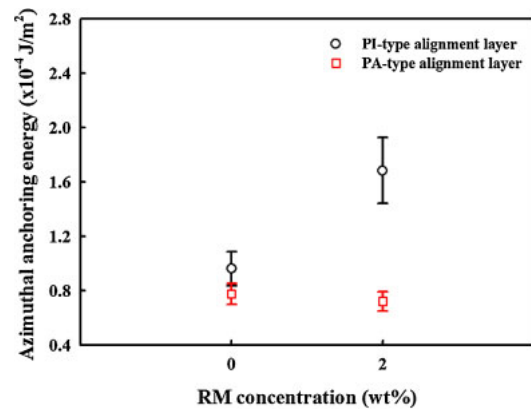


Fig. 2. (Color online) Measured azimuthal anchoring energy of two alignment layer types, both with and without the addition and UV curing of RMs. Open squares: PA-type alignment layer; open circles: PI-type alignment layer.

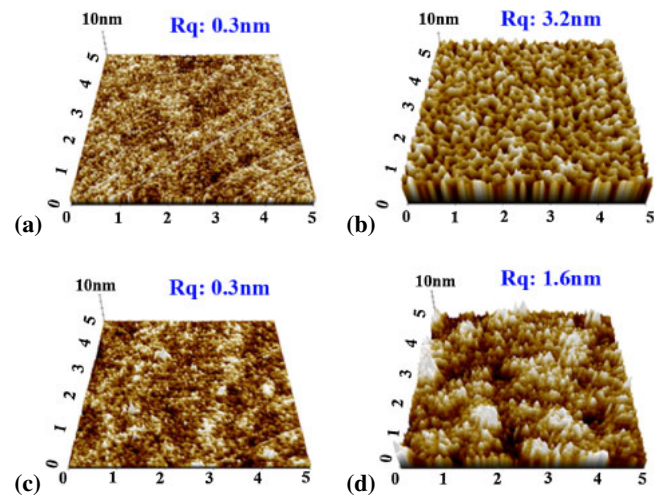


Fig. 3. (Color online) AFM micrographs of disassembled substrates: (a, b) PA-type and (c, d) PI-type alignment layers (a, c) without and (b, d) with RMs. R_q is the root-mean-square value of the surface roughness.

RM polymers on the surface of the alignment layer increased the azimuthal anchoring energy. Therefore, the presence of the RM polymers on the surface is the most important factor in understanding the ability of these polymers to enhance the azimuthal anchoring energy in the alignment layer.

To confirm these findings regarding the presence or absence of surface RM polymers, we removed LC molecules from the disassembled substrates by washing them with hexane, and analyzed the substrates' topographies by means of AFM. The aggregation and polymerization of RM monomers on a surface has been reported to form protrusions.¹⁶⁾ Such protrusions of RM were not found on either of the PA-type alignment layers [Figs. 3(a) and 3(b)], although their surface roughness was increased after washing. The same surface roughness effect was observed on both PI-type alignment layers [Figs. 3(c) and 3(d)], but protrusions of random peak height and size were formed on the whole area of the layer to which RMs had been added; these features were attributed to the presence of RMs on the surface. Lee et al. reported that RM monomers did not polymerize on the surface of the alignment layer when it had been covered with deionized

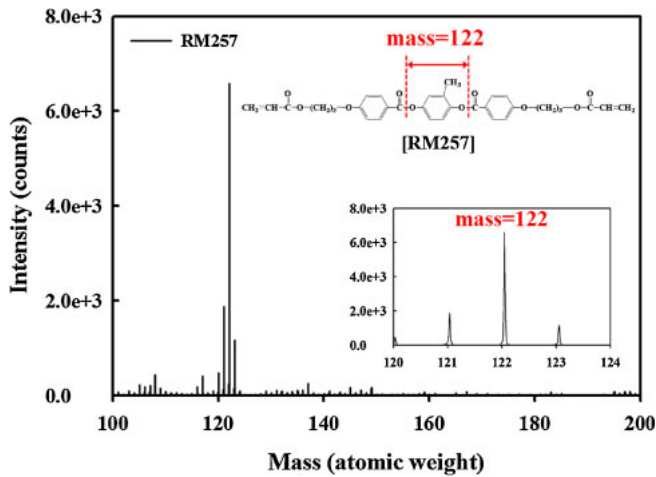
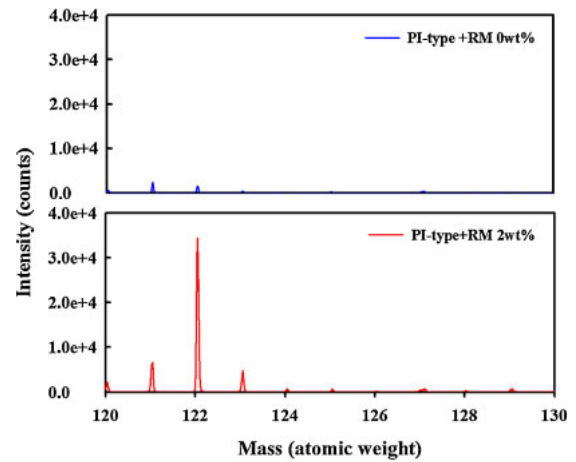


Fig. 4. (Color online) Secondary ion spectra of ITO glass coated with 0.7 wt% RMs dissolved in PGMEA, after UV exposure. Insert: molecular structure of RM257.

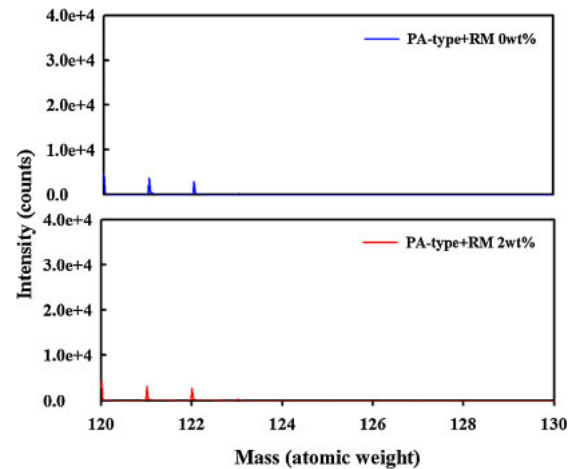
water, owing to the hydrophobicity of RM monomers.¹⁶⁾ In our system, the thermal imidization of the PA-type alignment layer entails a dehydration reaction between the polyamic acid and organic solvents (*N*-methyl-pyrrolidone and butylcellulose) at the surface during the thermal imidization process; this suggests that water generated near the alignment surface prevented the adhesion of RM monomers. In contrast, the PI-type alignment layer did not undergo imidization, and thus only organic solvents (*N*-methyl-pyrrolidone, butylcellulose, and butyrolactone) would have been present at the alignment surface; this would allow RM monomers to move freely in the out-of-plane direction because of their solubility in the organic solvents. Thus, the RM polymers on the surface could interact strongly with the LCs, thus enhancing the azimuthal anchoring energy.

To confirm that those protrusions are the polymerized RMs, surface mass analysis was carried out. To determine the characteristic TOF-SIMS response of RM257, we collected the secondary ion spectrum of ITO glass coated with 0.7 wt% RM dissolved in PGMEA and then exposed to UV (Fig. 4). The polymerized RM257 yielded a prominent peak corresponding to $C_7H_6O_2$ (mass: 122), the core group of RM257. Then, to confirm the presence or absence of RM polymers on the surface of the planar alignment layer to which RMs were added, TOF-SIMS surface mass analysis was conducted on four disassembled substrates, two each with PA- and PI-type alignment layers, and with or without the addition of polymerized RMs (Fig. 5). The addition of RM to the PI-type alignment layer yielded a high intensity peak at 122 mass, compared with the spectrum of the pure alignment layer [Fig. 5(a)]; however, no such difference was observed for the PA-type alignment layers with and without added RMs [Fig. 5(b)]. From these results, we concluded that the RM polymers were present on the surface of the PI-type alignment layer and not on the surface of the PA-type alignment layer, but rather in its bulk.

Surface analysis confirmed that the presence or absence of polymerized RMs on the surface of the alignment layer depended on the alignment material. Thus, the ability of the RMs to enhance the azimuthal anchoring energy depended on the alignment material used; the PI-type alignment layer was



(a)



(b)

Fig. 5. (Color online) Secondary ion spectra of disassembled substrates with and without added RMs: (a) PA- and (b) PI-type alignment layers.

more effective than the PA-type alignment layer in our proposed system.

The increased azimuthal anchoring energy affects the dynamic behavior of the FFS mode when an electric field is applied. The proposed relationship between the surface anchoring energy and the response time under a finite anchoring energy condition is as follows:⁹⁾

$$\tau_d = \frac{\gamma}{K_{22}\pi^2} \left(d^2 + \frac{4dK_{22}}{W} \right) \quad (1)$$

$$\tau_r = \frac{\tau_d}{|(V/V_{th})^2 - 1|}, \quad (2)$$

where

$$V_{th} = \pi \sqrt{\frac{K_{22}}{\epsilon_0 |\Delta \epsilon|}}.$$

In the above equations, W , d , γ , K_{22} , and V_{th} are the azimuthal anchoring energy, cell gap, rotational viscosity, twist elastic constant, and threshold voltage, respectively. It can be seen from the form of Eq. (1) that the decay time (τ_d) is improved by increasing the azimuthal anchoring energy. However, as can be seen from the form of Eq. (2), the rising time characteristics are more complicated to explain than the decay time; the rising time (τ_r) depends on the voltage

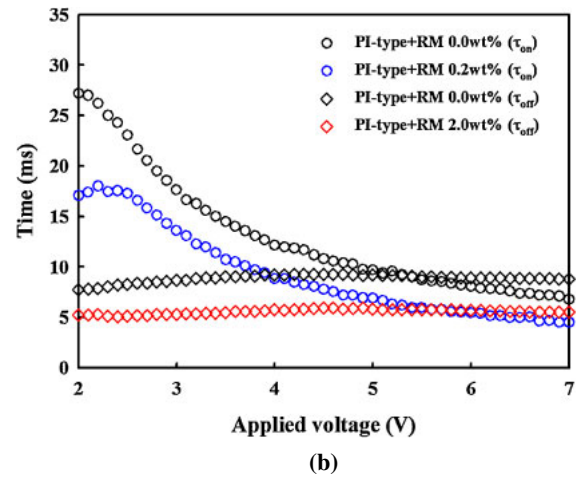
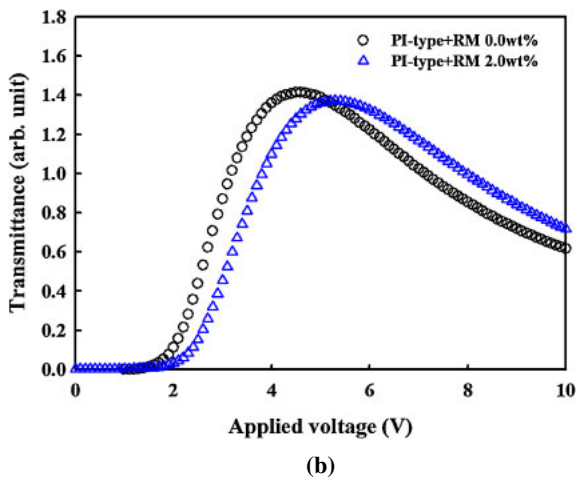
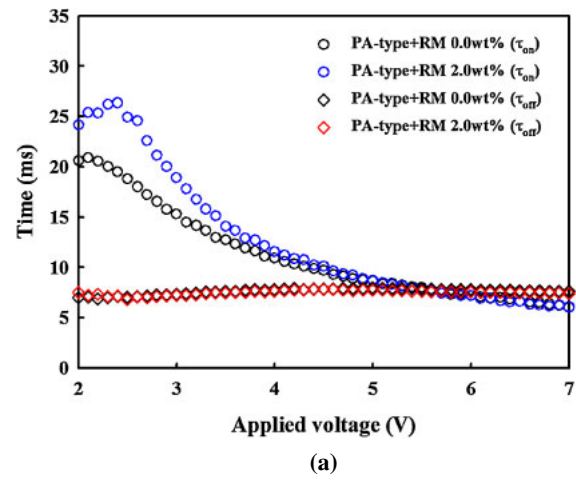
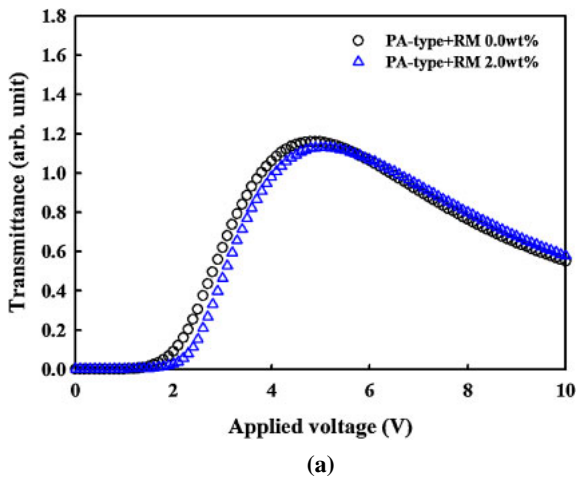


Fig. 6. (Color online) Measured voltage–transmittance characteristics of FFS cells without and with RMs: (a) PA- and (b) PI-type alignment layers.

Fig. 7. (Color online) Measured voltage–response time characteristics of FFS cells without and with RMs: (a) PA- and (b) PI-type alignment layers.

switching ratio, defined as V/V_{th} for a given LC material and cell gap.¹⁷⁾

Figure 6 shows the transmittance of the FFS mode as a function of applied voltage for the PA- and PI-type alignment layers, with and without RMs. In case of the PA-type alignment layer, the inclusion of RMs shifted the transmittance–voltage curve to the right, and the threshold voltage (V_{th}), which was inversely proportional to the square of the rising time, was also increased. However, the voltage switching ratio (V/V_{th}) was not increased, owing to a simultaneous increase in the on-state voltage compared to that of the pure alignment layer, as shown in Fig. 6(a). In contrast, for the PI-type alignment layer to which RMs were added, the voltage switching ratio was increased because the change of the on-state voltage was larger than the change in the threshold voltage, as shown in Fig. 6(b). This higher voltage switching ratio was the cause of the fast rising time characteristics observed.

Figure 7 shows the response time characteristics of the various cells as a function of applied voltage. As we expected, in the PA-type alignment layers, the addition of RMs did not produce remarkable improvement in the response time because it did not greatly affect the azimuthal anchoring energy or the voltage switching ratio [Fig. 7(a)]; however, the addition of RMs to the PI-type alignment layer improved the decay time as well as the FFS mode rising time

characteristics over the entire region of applied voltage, as shown in Fig. 7(b). The fast decay time of the PI-type cell resulted from the strong increase in azimuthal anchoring energy caused by the presence of the RM polymer on the surface of the alignment layer. The fast rising time characteristics resulted from the strong dielectric torque based on the high order parameter, as reported in our previous paper,¹⁸⁾ and the higher voltage switching ratio, as mentioned above.

4. Conclusions

We reported the addition of RMs to a planar alignment layer to improve its azimuthal anchoring energy. The addition of RMs to a PI-type alignment surface, and their subsequent UV polymerization, considerably increased the azimuthal anchoring energy by increasing the chain ordering and strengthening molecular interactions. In contrast, the addition of RMs to a PA-type alignment layer was ineffective because the thermal imidization of PA prevented surface adhesion of the hydrophobic RMs. Surface properties were analyzed by AFM and TOF-SIMS. Strong azimuthal anchoring energy increased the response speed of cells operating in the FFS mode. We believe that this method is applicable for improving the response time characteristics of various LC devices, and will be helpful in the further development of planar alignment materials for FFS-mode and IPS-mode operation.

Acknowledgments

This work was supported by the National Research Foundation of Korea (NRF) funded by the Ministry of Education, Science, and Technology of Korean Government (MEST) (2012R1A2A2A01046967) and Samsung Electronics Co., Ltd.

- 1) S. Oka, T. Mitsumoto, M. Kimura, and T. Akahane, *Phys. Rev. E* **69**, 061711 (2004).
- 2) J.-H. Kim and C. Rosenblatt, *J. Appl. Phys.* **84**, 6027 (1998).
- 3) B. Jérôme, *Rep. Prog. Phys.* **54**, 391 (1991).
- 4) M. I. Boamfa, M. W. Kim, J. C. Maan, and Th. Rasing, *Nature* **421**, 149 (2003).
- 5) A. Rapini and M. Papoular, *J. Phys. Colloq.* **30**, C4-54 (1969).
- 6) O. Yaroshchuk, V. Kyrychenko, D. Tao, V. Chigrinov, H. S. Kwok, H. Hasebe, and H. Takatsu, *Appl. Phys. Lett.* **95**, 021902 (2009).
- 7) K.-W. Lee, S.-H. Paek, A. Lien, C. Durning, and H. Fukuro, *Macromolecules* **29**, 8894 (1996).
- 8) L. Komitov, *Thin Solid Films* **516**, 2639 (2008).
- 9) X. Nie, R. Lu, H. Xianyu, T. X. Wu, and S.-T. Wu, *J. Appl. Phys.* **101**, 103110 (2007).
- 10) M. J. Escuti, C. C. Bowley, G. P. Crawford, and S. Zumer, *Appl. Phys. Lett.* **75**, 3264 (1999).
- 11) Y. J. Lim, C. W. Woo, S. H. Oh, A. Mukherjee, S. H. Lee, J. H. Baek, K. J. Kim, and M. S. Yang, *J. Phys. D* **44**, 325403 (2011).
- 12) Y.-K. Moon, M.-G. Choi, T.-M. Kim, J.-H. Jeong, Y.-J. Lee, C.-J. Yu, and J.-H. Kim, Proc. 17th Int. Display Workshop, 2010, p. 23.
- 13) Y. Saitoh and A. Lien, *Jpn. J. Appl. Phys.* **39**, 1743 (2000).
- 14) B. R. Acharya, J.-H. Kim, and S. Kumar, *Phys. Rev. E* **60**, 6841 (1999).
- 15) Y.-K. Moon, Y.-J. Lee, S. I. Jo, Y. Kim, J. U. Hae, J.-H. Baek, S.-G. Kang, C.-J. Yu, and J.-H. Kim, *J. Appl. Phys.* **113**, 234504 (2013).
- 16) Y.-J. Lee, C.-J. Yu, Y.-K. Kim, S. I. Jo, and J.-H. Kim, *Appl. Phys. Lett.* **98**, 033106 (2011).
- 17) M. Jiao, Z. Ge, Q. Song, and S.-T. Wu, *Appl. Phys. Lett.* **92**, 061102 (2008).
- 18) Y. Kim, Y.-J. Lee, D.-H. Kim, J.-H. Baek, J.-H. Lee, B.-K. Kim, C.-J. Yu, and J.-H. Kim, *J. Phys. D* **46**, 485306 (2013).